New light particle searches with PADME

Kalina Dimitrova
Faculty of Physics, Sofia University

Workshop at 1GeV scale: From mesons to axions

19-20.09.2024
Krakow, Poland

* *partially supported by **BNSF: KP-06-D002_4/15.12.2020** within **MUCCA, CHIST-ERA-19-XAI-009***

Outline

- The PADME Experiment: detectors and data taking

- PADME Run I and Run II
  - Results on e+e– → γγ cross section

- PADME Run III
  - Setup and strategy for X17 search
  - Signal and event selection
  - Sensitivity estimation

- Towards PADME Run IV

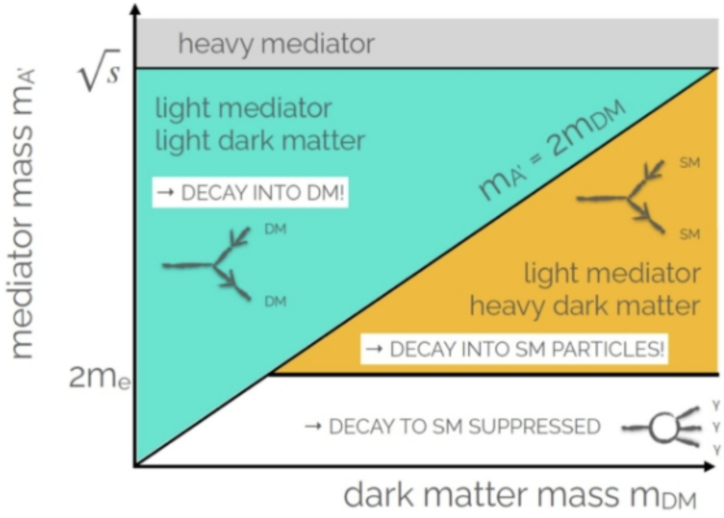

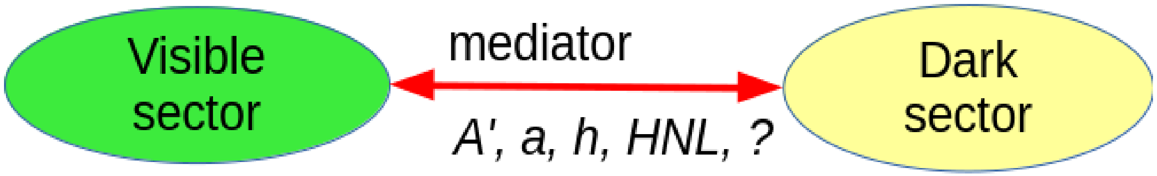

Positron annihilation into new light particles

Associated production: $e^+ e^- \rightarrow A' \gamma$

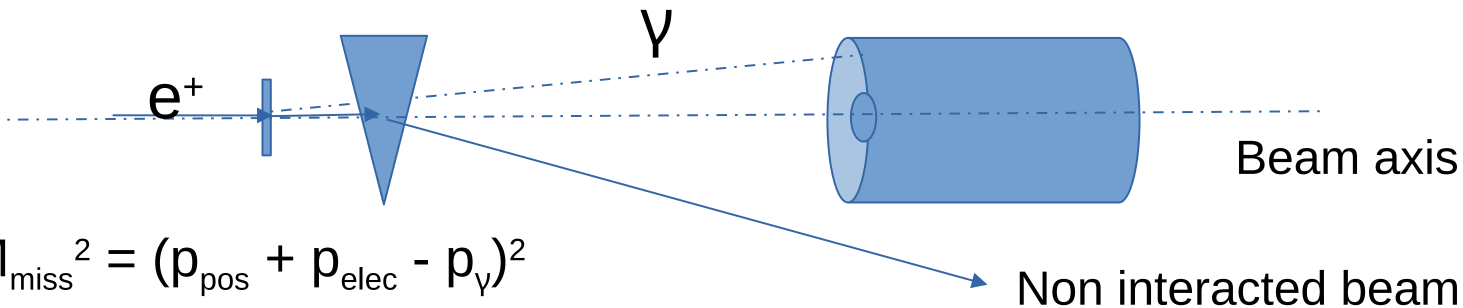

$$M_{miss}^2 = (p_{pos} + p_{elec} - p_{\gamma})^2$$

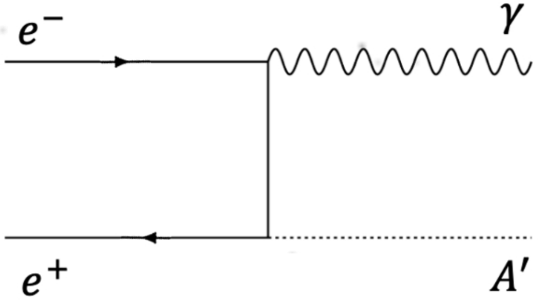

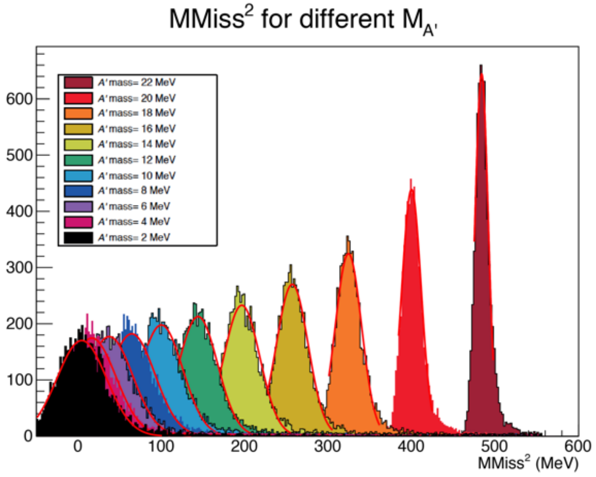

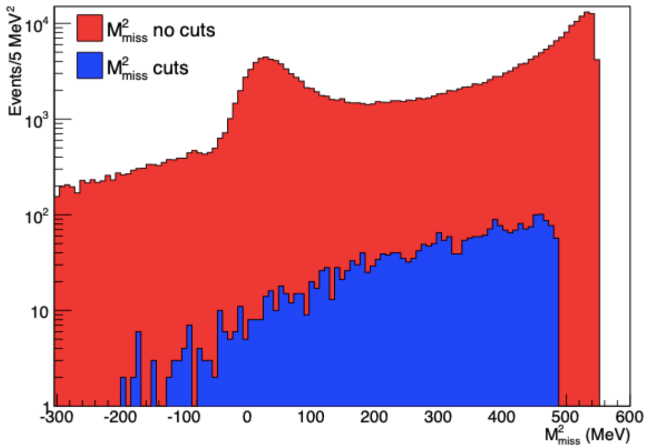

The PADME technique

Small scale experiment @ Frascati Beam Test Facility

Combination of fixed target and collider techniques

Annihilation of accelerated antiparticles with matter

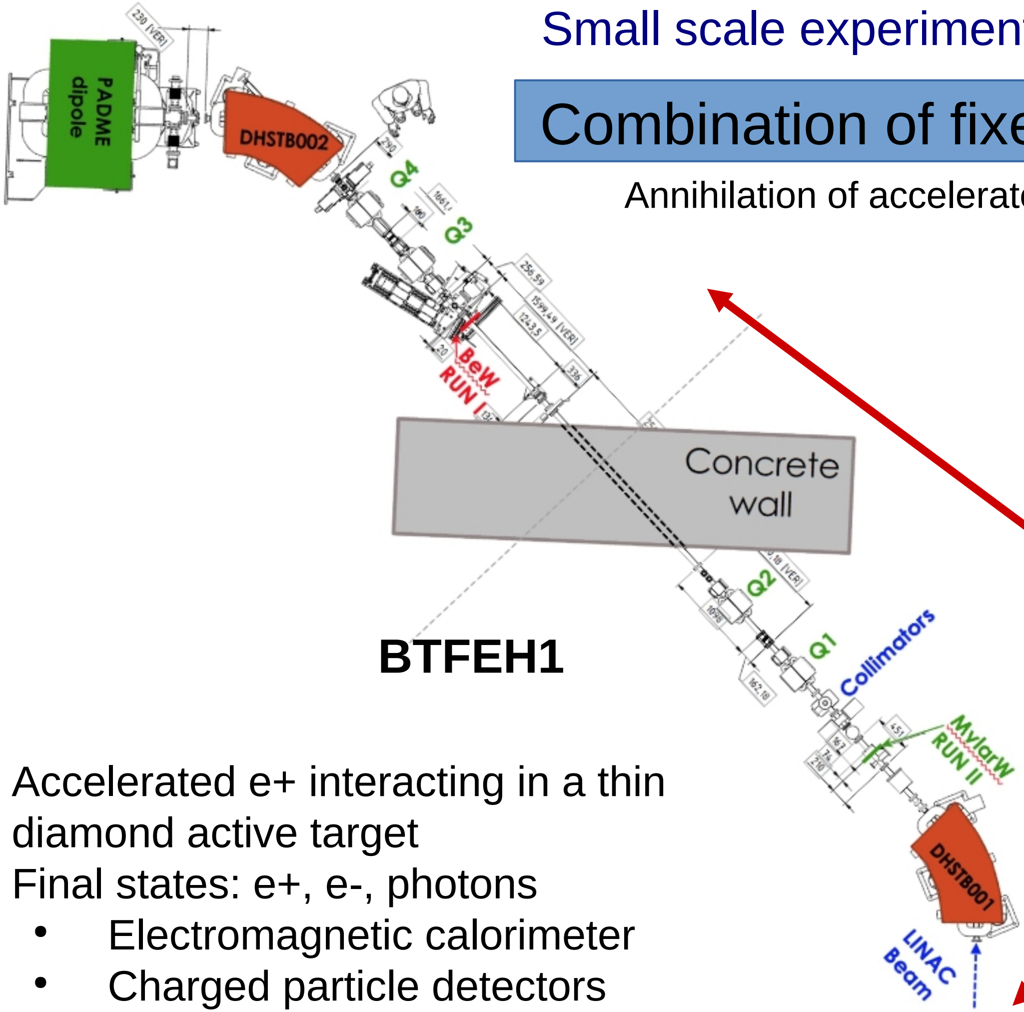

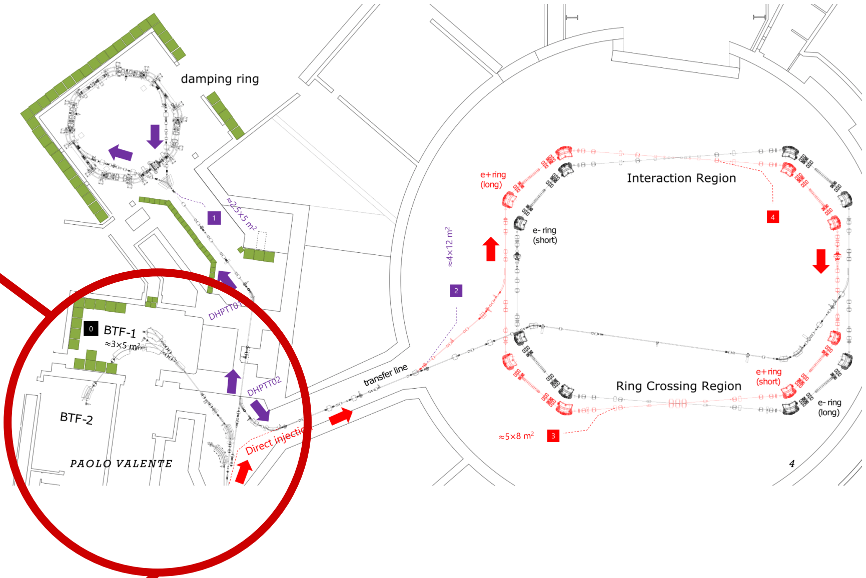

- Accelerated e+ interacting in a thin diamond active target
- Final states: e+, e-, photons
  - Electromagnetic calorimeter
  - Charged particle detectors

PADME Experiment

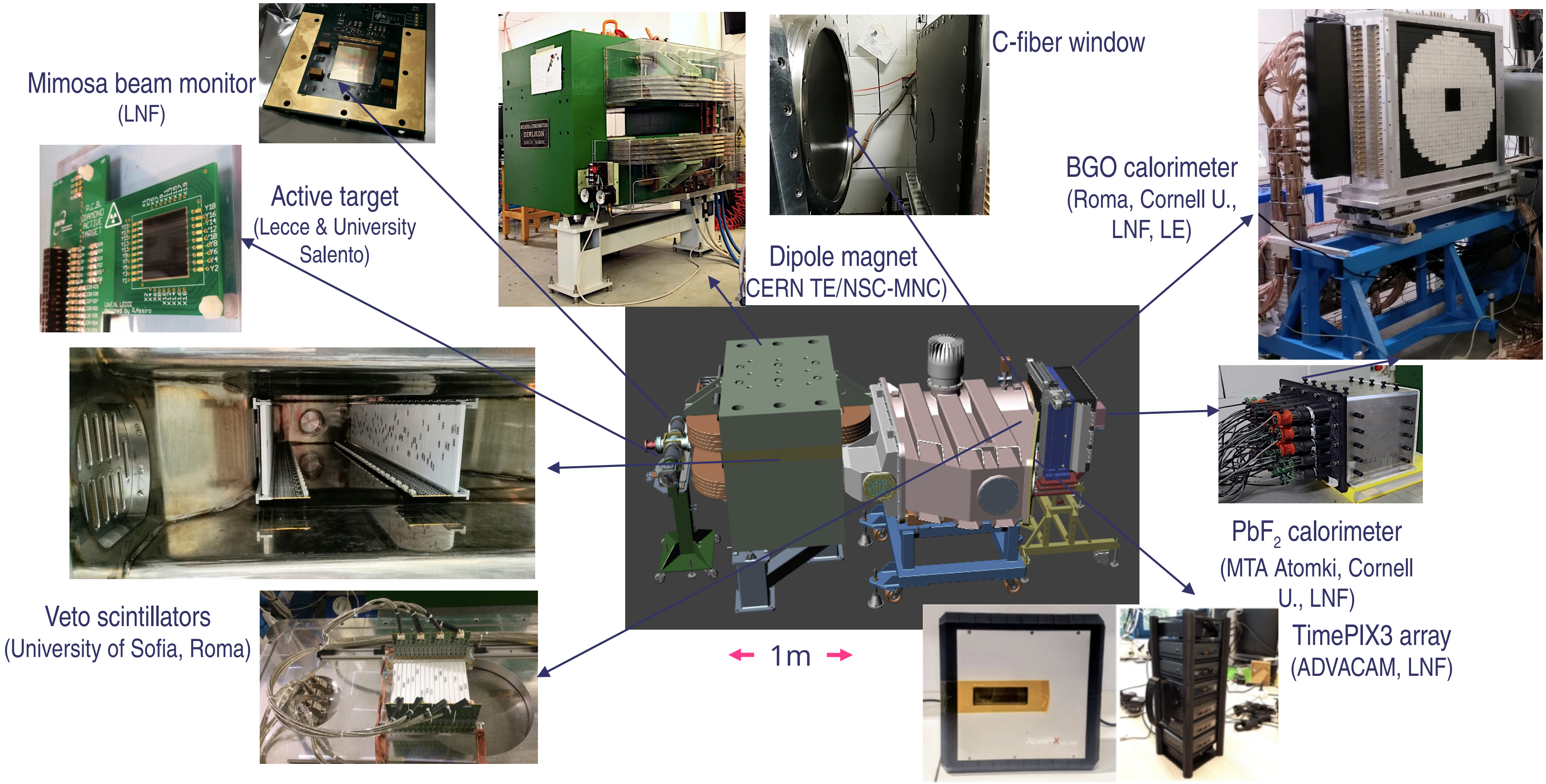

Active target

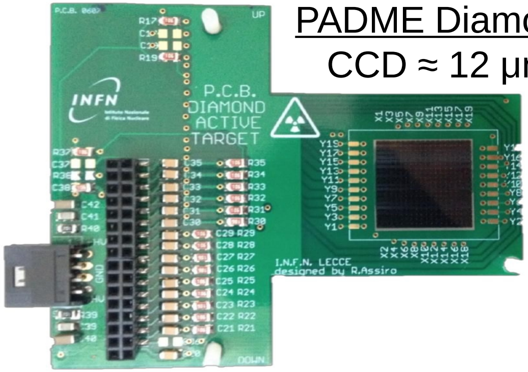

PADME Diamond
CCD ≈ 12 μm

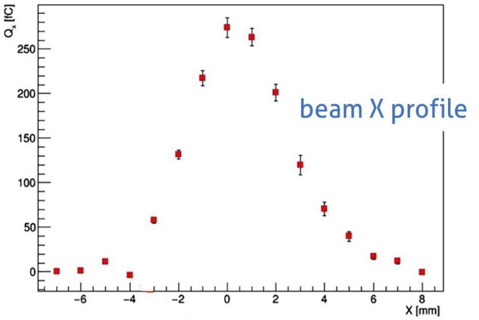

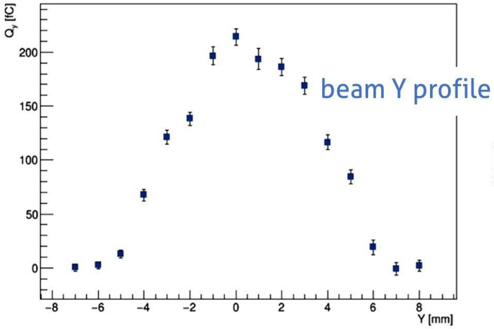

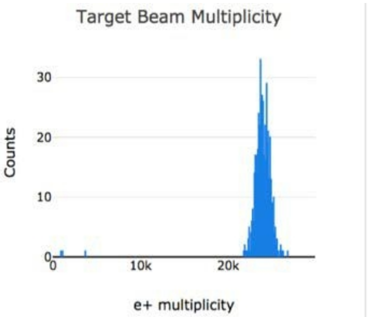

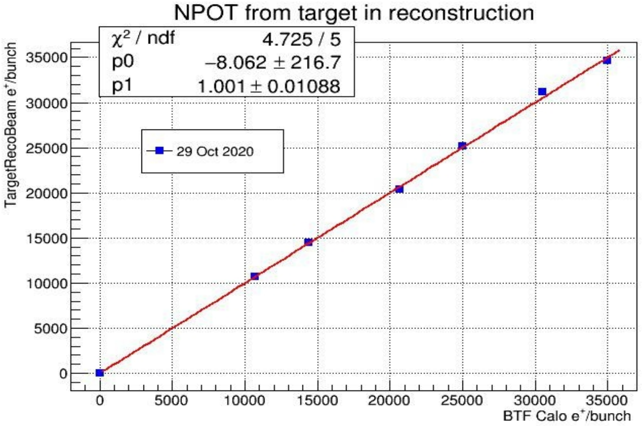

- **Polycrystalline diamond**
- 100 μm thickness:
- 16 × 1 mm strip and X-Y readout in a single detector
- Graphite electrodes using excimer laser

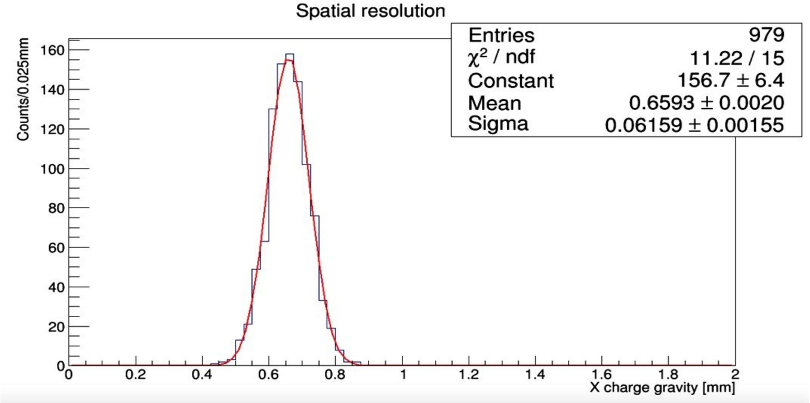

- *JINST* 12 (2017) 02, C02036

Calorimeters

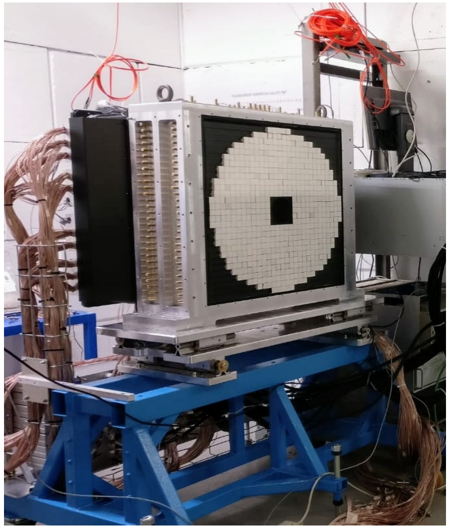

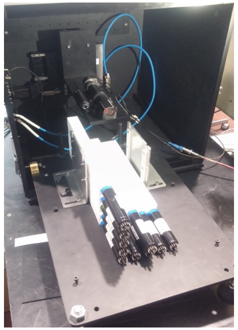

ECAL: The heart of PADME

- 616 BGO crystals, 2.1 x 2.1 x 23 cm^3
- BGO covered with diffuse reflective TiO_2 paint
  - additional optical isolation: 50 – 100 µm black tedlar foils

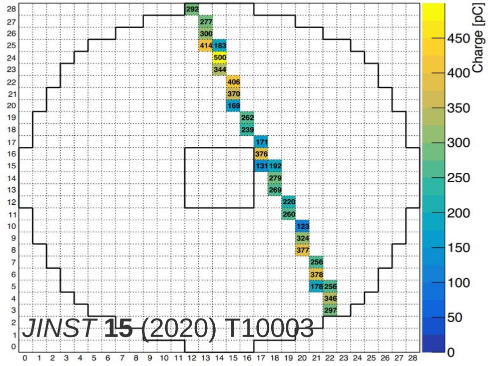

JINST **15** (2020) T10003

Calibration at several stages:

- BGO + PMT equalization with ^{22}Na source before construction
- Cosmic rays calibration using the MPV of the spectrum
- Temperature monitoring

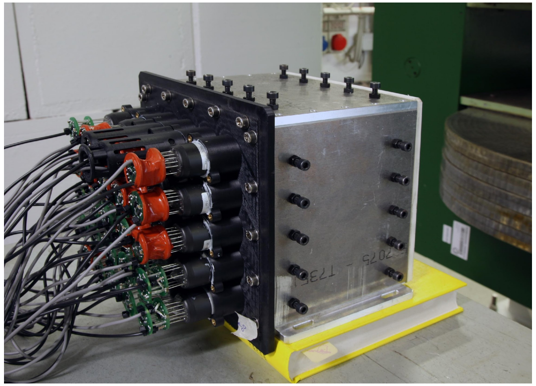

Nucl.Instrum.Meth.A 919 (2019) 89-97

Small Angle Calorimeter (SAC)

- 25 crystals - 5 x 5 matrix, Cherenkov PbF_2
- Dimensions of each crystal: 3 × 3 × 14 cm^3
- 50 cm behind ECal
- PMT readout: Hamamatsu R13478UV with custom dividers
- Angular acceptance: [0,19] mrad

Recorded bunch

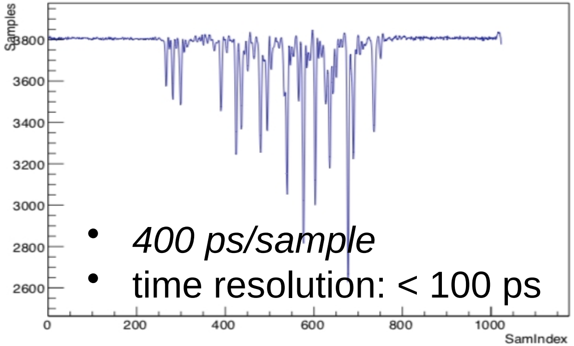

- *400 ps/sample*
- time resolution: < 100 ps

Charged particle detectors

- Three sets of detectors detect the charged particles from the PADME target (at E_{beam} = 550 MeV):
  - **PVeto**: positrons with 50 MeV < p_{e+} < 450 MeV
  - **HEPVeto**: positrons with 450 MeV < p_{e+} < 500 MeV
  - **EVeto**: electrons with 50 MeV < p_{e+} < 450 MeV
- 96 + 96 (90) + 16 (x2)   scintillator-WLS-SiPM RO channels
- Segmentation provides momentum measurement down to ~ 5 MeV resolution

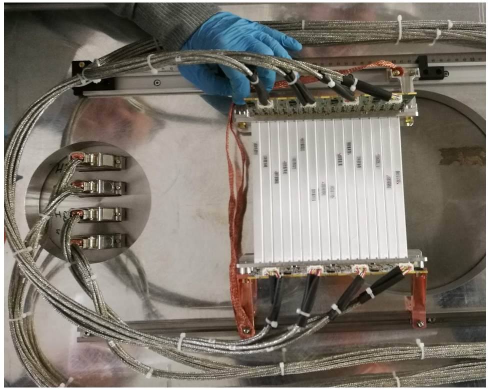

Time calibration with SAC using Bremsstrahlung events

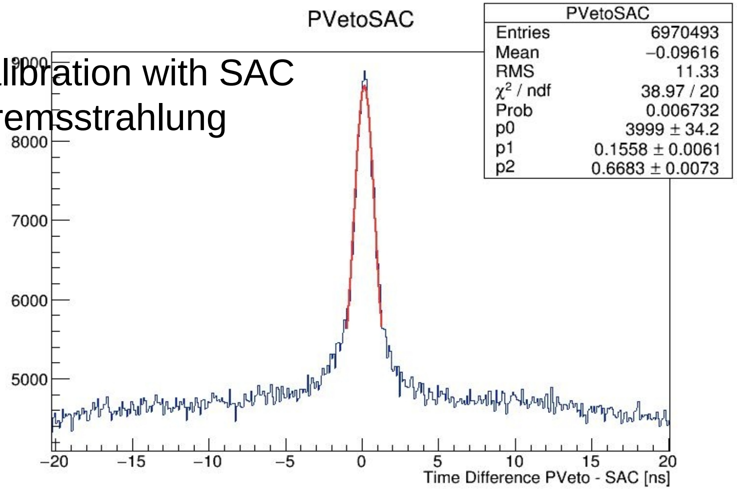

- Custom SiPM electronics, Hamamatsu S13360 3 mm, 25µm pixel SiPM
- Differential signals to the controllers, HV, thermal and current monitoring

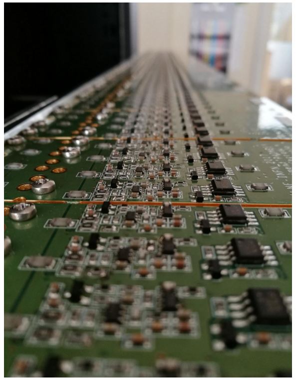

JINST 19 (2024) 01, C01051

- Online time resolution: ~ 2 ns
- Offline time resolution after fine T_0 calculation – better than 1 ns

Main background processes

- **Bremsstrahlung in the field of the target nuclei**
  - Photons mostly @ low energy, background dominates the high missing masses
  - An additional lower energy positron that could be detected due to stronger deflection
- **2 photon annihilation**
  - Peaks at $M_{miss} = 0$
  - Quasi symmetric in gamma angles for $E_{\gamma} > 50$ MeV
- **3 photon annihilation**
  - Symmetry is lost – decrease in the vetoing capabilities
- **Radiative Bhabha scattering**
  - Topology close to bremsstrahlung

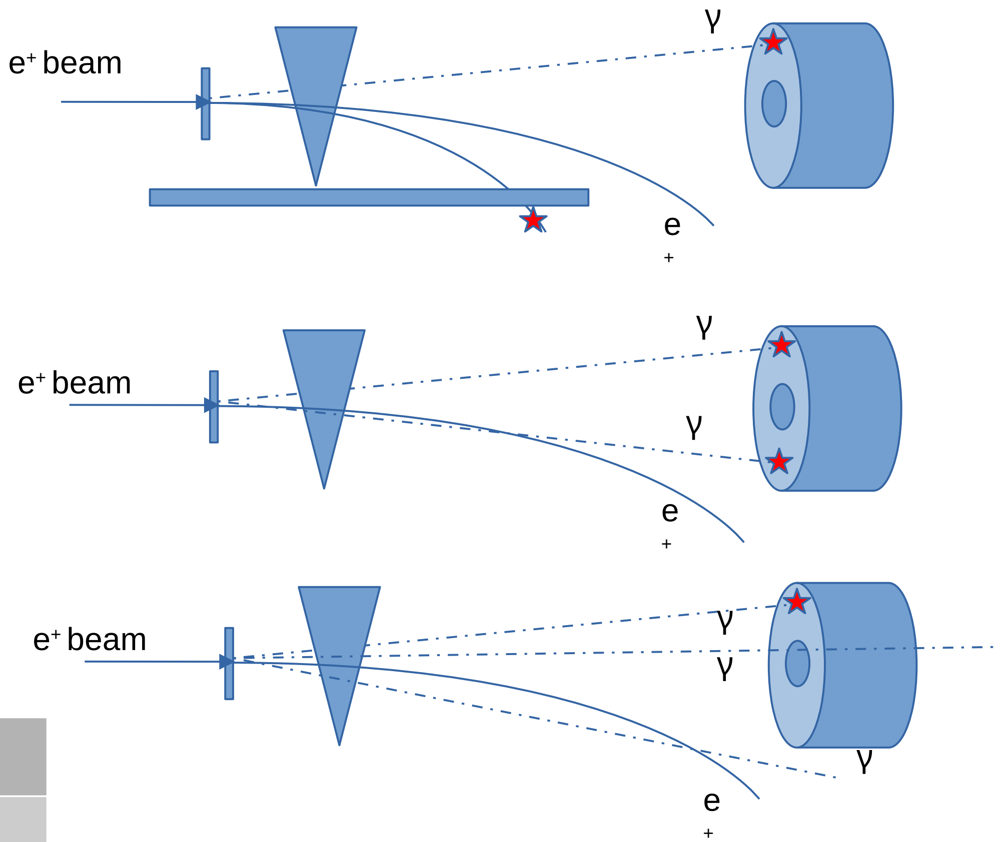

Background process	Cross section e^+@550 MeV beam	Comment *Carbon target*
$e^+e^- \rightarrow \gamma\gamma$	1.55 mb	
$e^+ + N \rightarrow e^+ N \gamma$	4000 mb	$E\gamma > 1$MeV
$e^+e^- \rightarrow \gamma\gamma\gamma$	0.16 mb	CalcHEP, $E\gamma > 1$MeV
$e^+e^- \rightarrow e^+e^-\gamma$	180 mb	CalcHEP, $E\gamma > 1$MeV

PADME RUN I and II

Run I and PADME commissioning

- started in Autumn 2018 and ended on February 25th
  - ~7 x 10^{12} PoT recorded with secondary beam
  - PADME DAQ, Detector, beam, collaboration commissioning
  - Data quality and detector calibration
- PADME test beam data
  - July 2019, few days of valuable data
    - Certification of the primary beam
  - Detector performance/calibration checks
  - Primary beam with E_{beam} = 490 MeV

RUN II: primary beam

- July 2020
  - New environment/detector parameter monitoring and control system
  - Remote operation confirmation
- Autumn 2020:
  - A long data taking period with O(5x10^{12}) e^+ on target
  - E_{beam} = 430 MeV

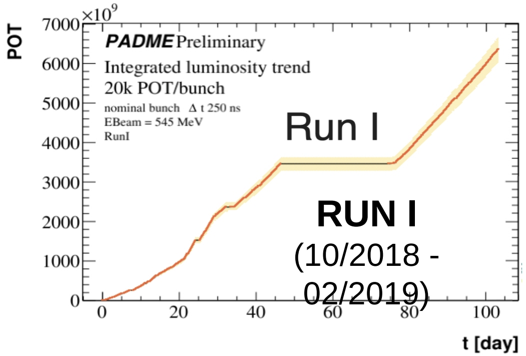

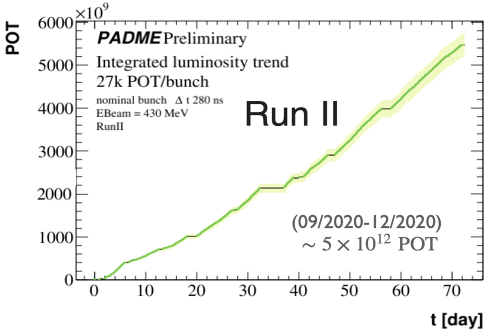

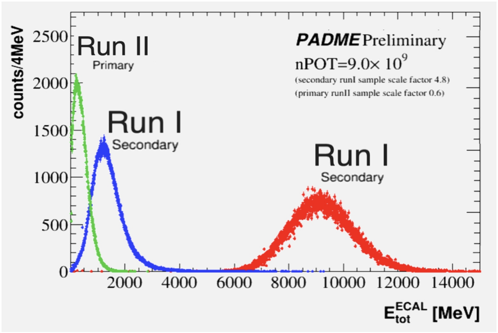

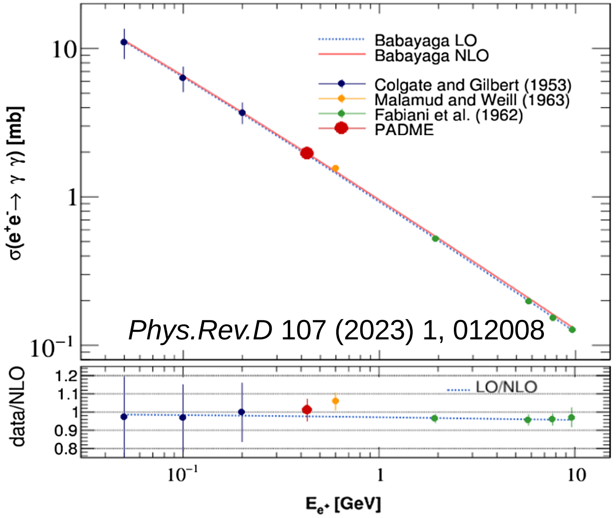

ML for double particle separation in ECal

Instruments 6 (2022) 4, 46

PADME ECAL

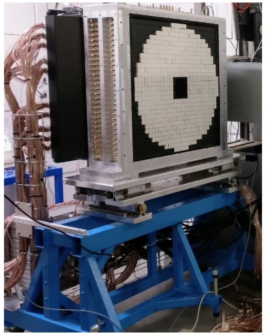

Two photon showers
in the ECAL

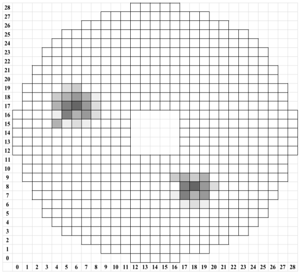

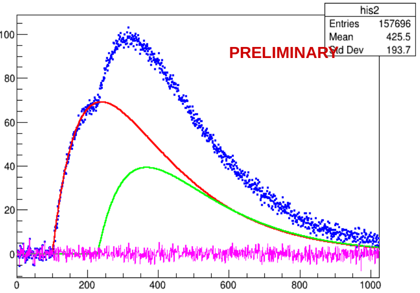

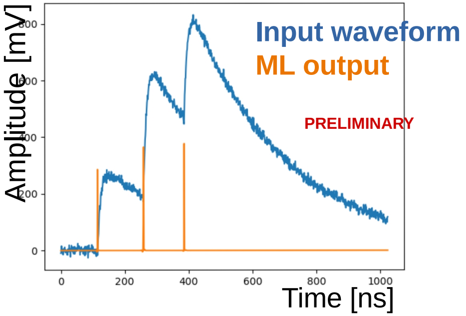

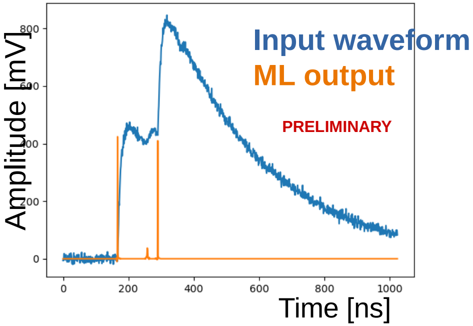

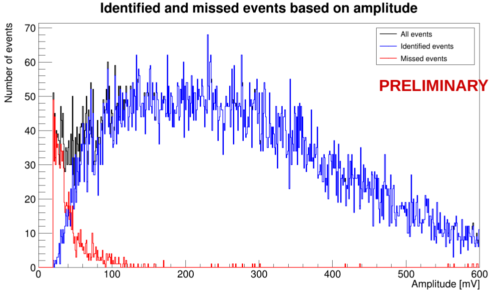

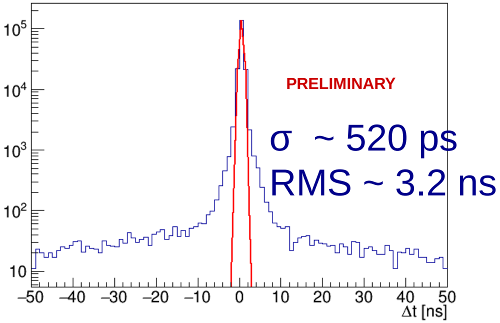

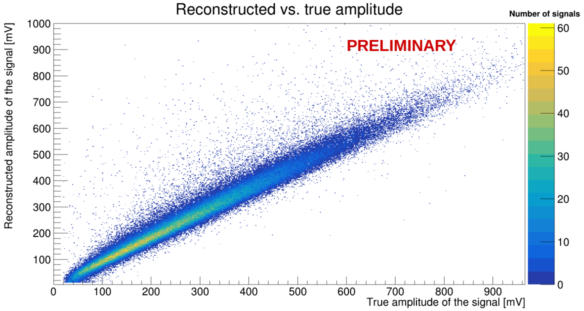

- AI to identify the number of pulses in a waveform
- Simple output – up to five pulses
- Trained on 100 000 events

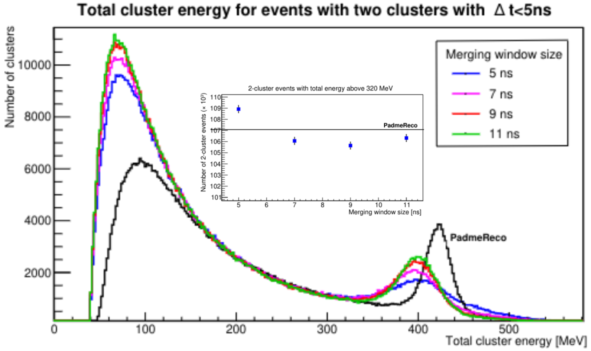

e+e– → γγ events

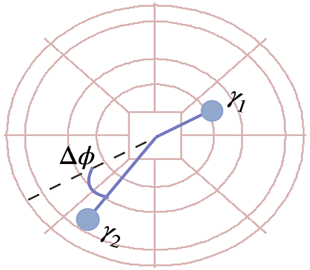

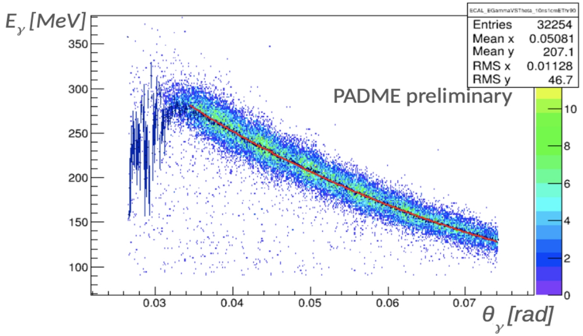

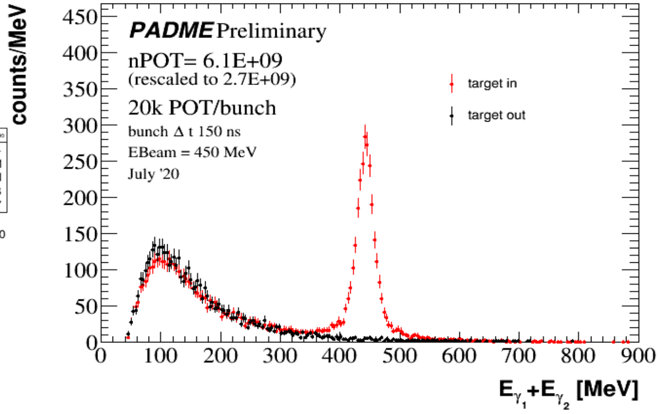

e+e− → γγ cross section

- Below 0.6 GeV known only with 20% accuracy
- Can be sensitive to sub-GeV new physics (e.g. ALP's)
- Using 10% of Run II sample
- Tag-and-probe method on two back-to-back clusters
- Exploit energy-angle correlation

Tag photons selection

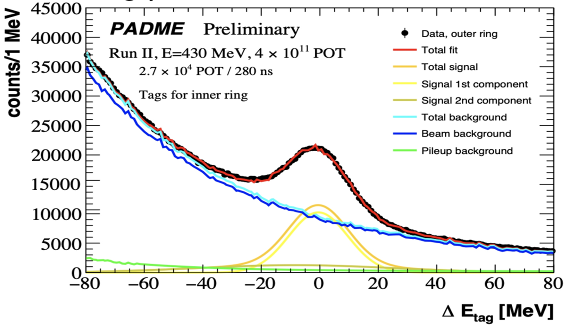

Probe photons

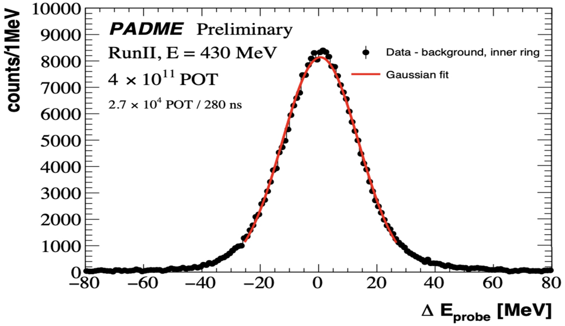

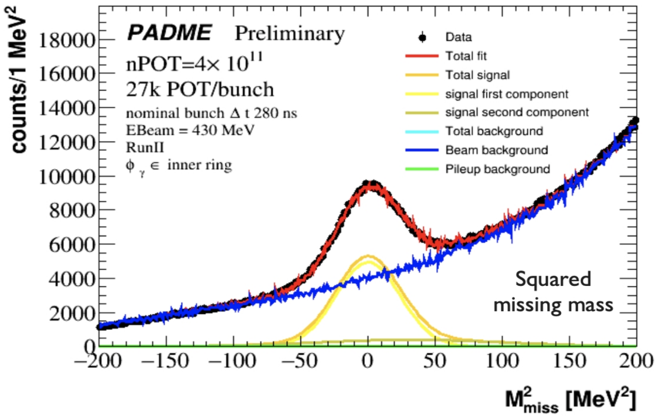

e+e– → γγ cross section

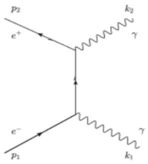

LO

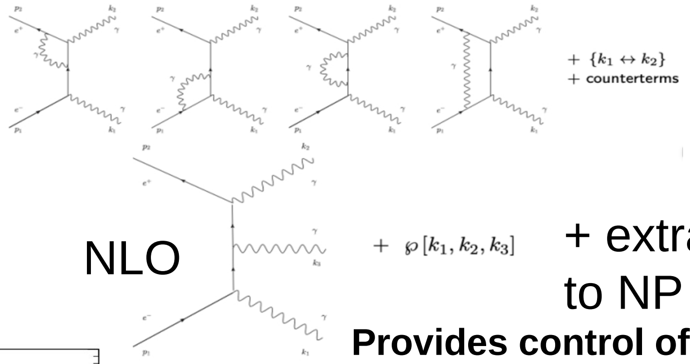

NLO

+ extra due to NP

Provides control of the e⁺ flux

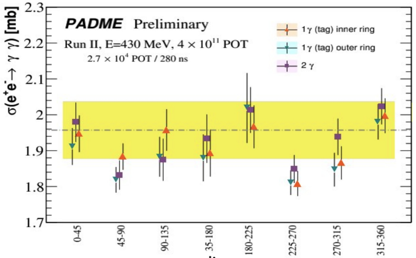

φ slice

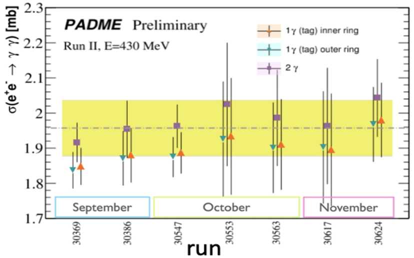

run

Systematic effect	**Contribution δ [mb]**
Detector response uniformity	0.020
Background modelling	0.047
Acceptance	0.025
n POT: target calibration	0.079
Electron density (target thickness)	0.020

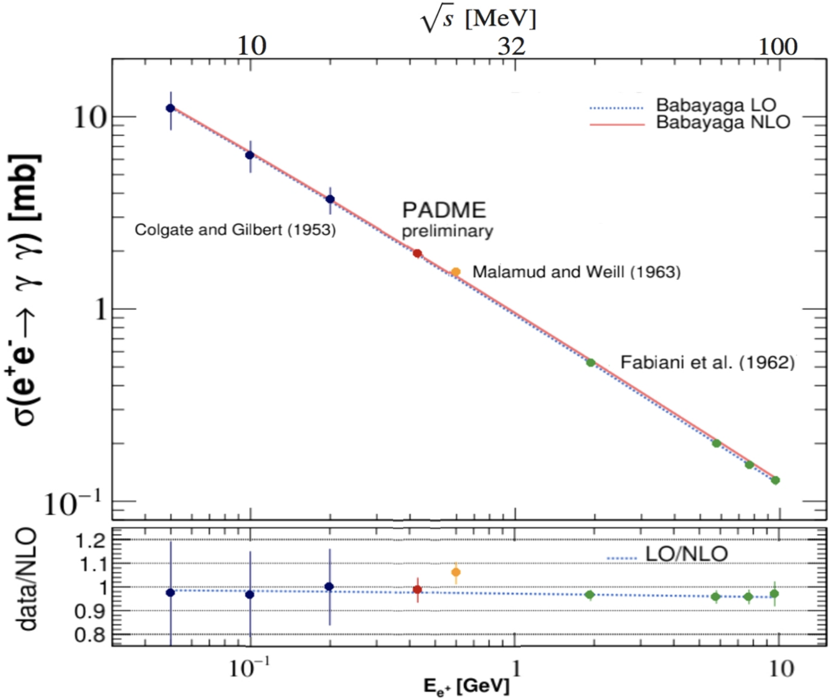

$$\sigma(e^+e^- \to \gamma\gamma(\gamma)) = 1.930 \pm 0.029(\text{stat}) \pm 0.099(\text{syst})\ \text{mb}$$

Probing X17

PRL 116 (2016) 042501

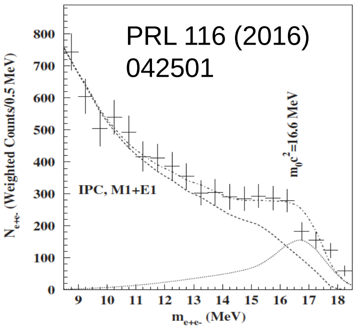

Phys.Rev.C 104, 044003 (2021)

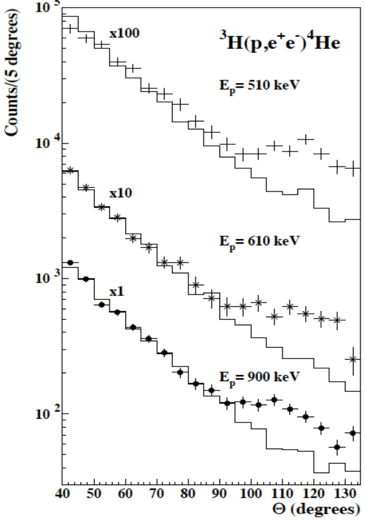

Phys. Rev. C 106, L061601 (2022)

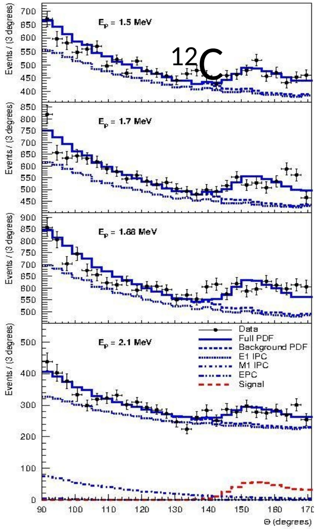

2022

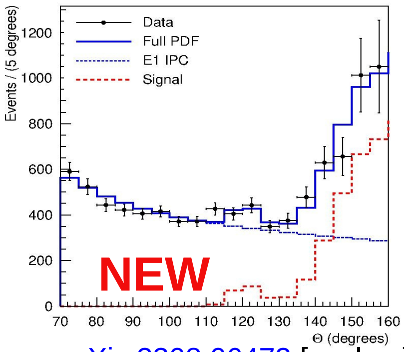

arXiv:2308.06473 [nucl-ex]

Phys. Rev. D 101, 071101(R)

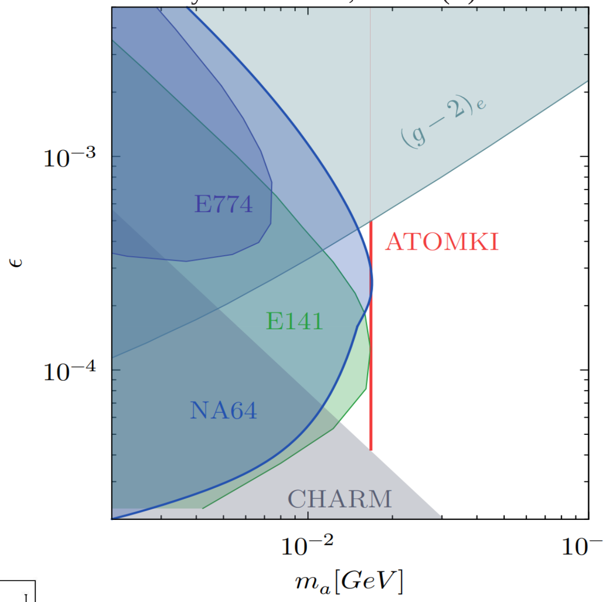

arXiv:2104.13342 [hep-ex]

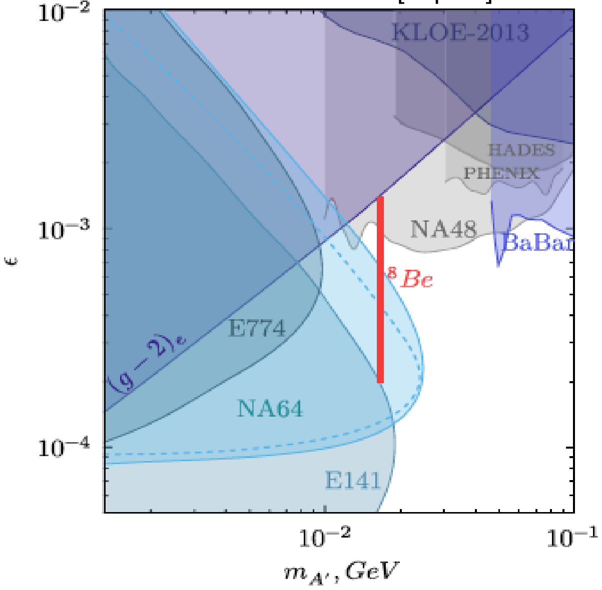

- Similar physics observables as in the ^{8}Be, ^{4}He and ^{12}C experiments
  - 2 leptons in the final state
  - Kinematics properties determined by the mass of the X particle (2 body decays)

PADME strategy for X17

Cross section enhancement with the approach of the production threshold

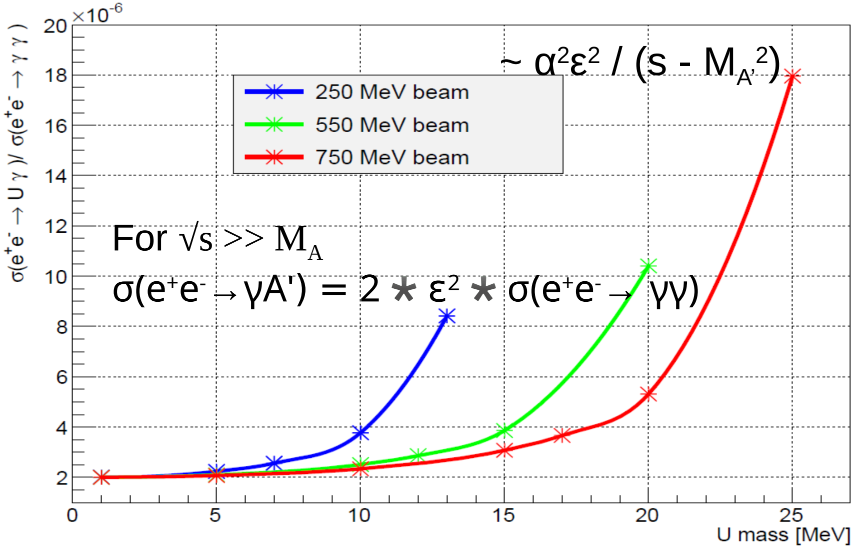

L. Darmé et. al.,

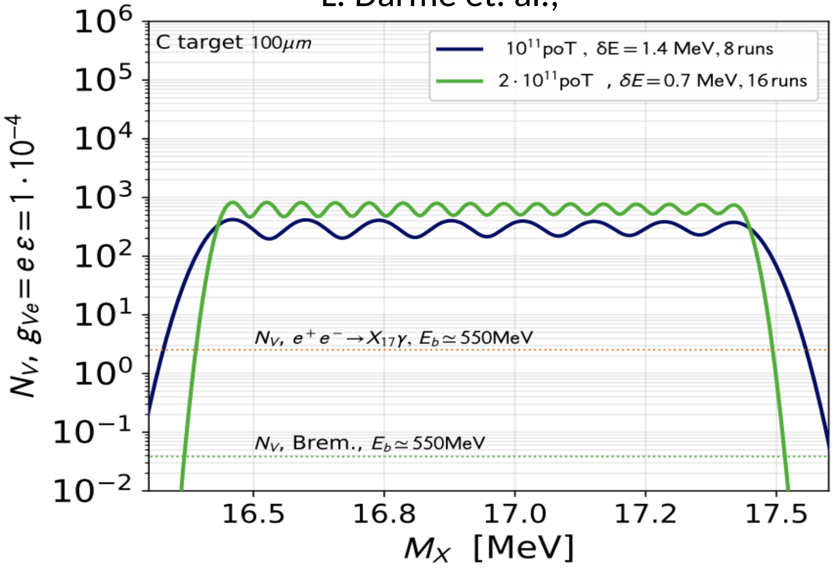

- Resonant production of X17
- Energy at resonance: ~283 MeV: scan
- Need to measure the final state to reconstruct the invariant mass
  - Or change in cross section

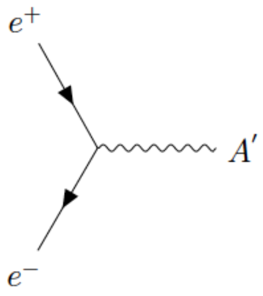

$$\sigma_{\rm res}(E_e) = \sigma_{\rm peak}\frac{\Gamma_{A'}^2/4}{(\sqrt{s}-m_{A'})^2+\Gamma_{A'}^2/4}$$

$$\sigma_{\rm peak} = 12\pi/m_{A'}^2 \qquad \Gamma_{A'} = \frac{1}{3}m_{A'}\varepsilon^2\alpha$$

e+e- → X17 → e+e-

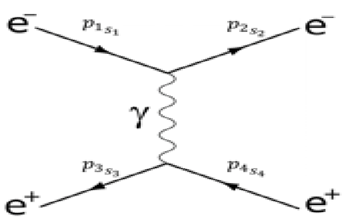

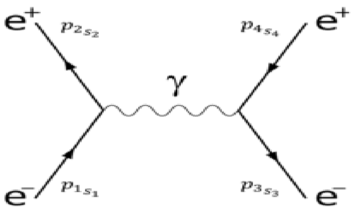

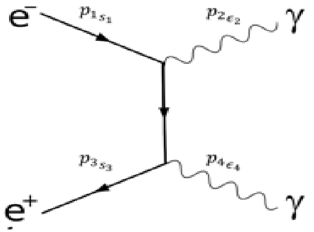

Bhabha scattering dominates the event rate in the background contribution for high P_{e+}

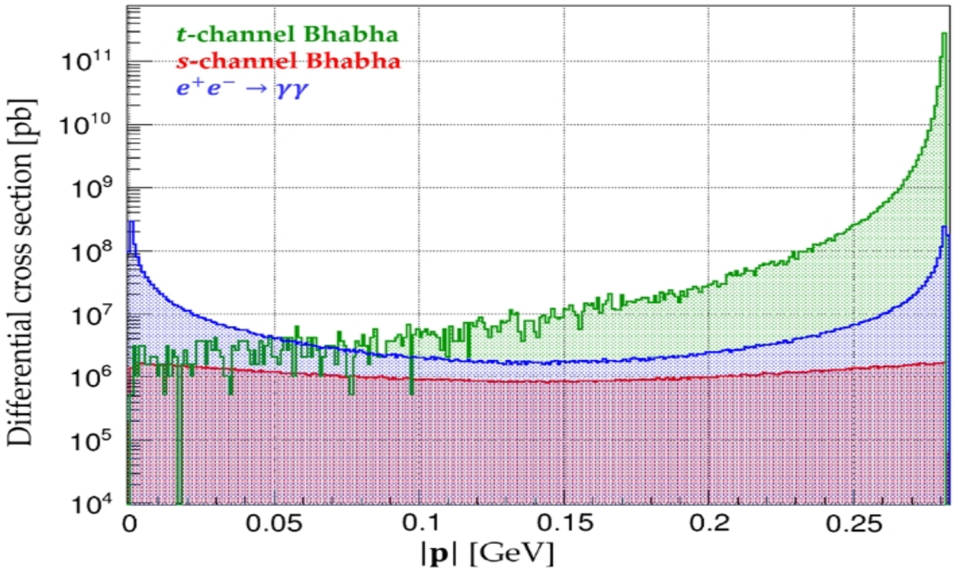

Resonant cross section significant → X17 event yield

$$\mathcal{N}_{X_{17}}^{\text{Vect.}} \simeq 1.8 \cdot 10^{-7} \times \left(\frac{g_{ve}}{2 \cdot 10^{-4}}\right)^2 \left(\frac{1\ \text{MeV}}{\sigma_E}\right)$$

$$\mathcal{N}_{X_{17}}^{\text{ALP}} \simeq 5.8 \cdot 10^{-7} \times \left(\frac{g_{ae}}{\text{GeV}^{-1}}\right)^2 \left(\frac{1\ \text{MeV}}{\sigma_E}\right)$$

σ_E - beam energy spread

Production of O(10^3) X17 events with 10^{10} positrons on target

Change in $\sigma_{tot}(e^+e^- \rightarrow e^+e^-)$

PADME RUN III

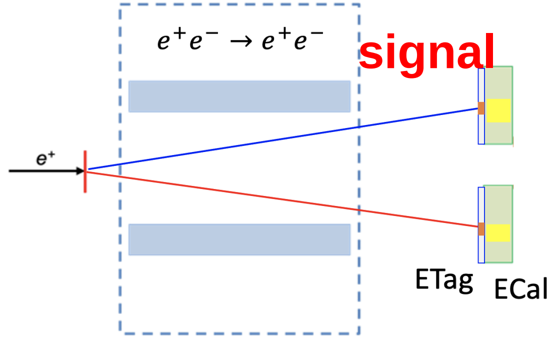

Running with no magnetic field in PADME dipole

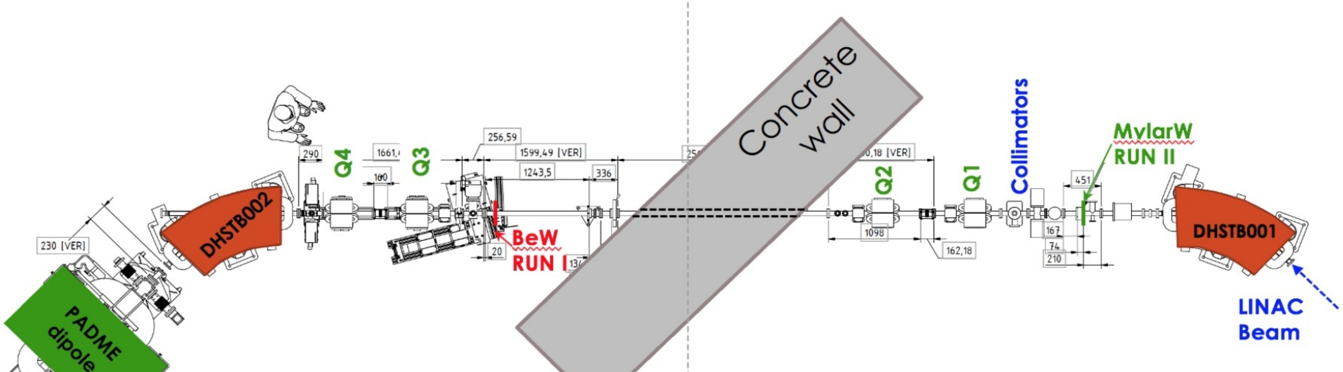

Measuring N_{e+e-} /F (E_{beam}), F – the total flux of positrons

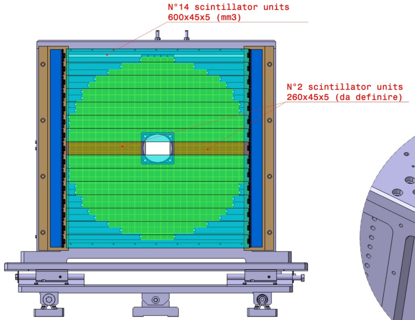

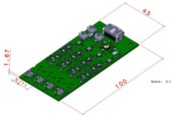

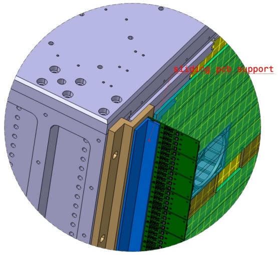

Components in the analysis:

- **Signal selection & events identification**
  - Background contribution
- **Determination of the normalization**
  - PADME beam measurement
- **Expected signal yield**
  - “Theory” input: X17 line shape

Signal selection: $N_{2cl} = N_{e+e-} + N_{\gamma\gamma}$

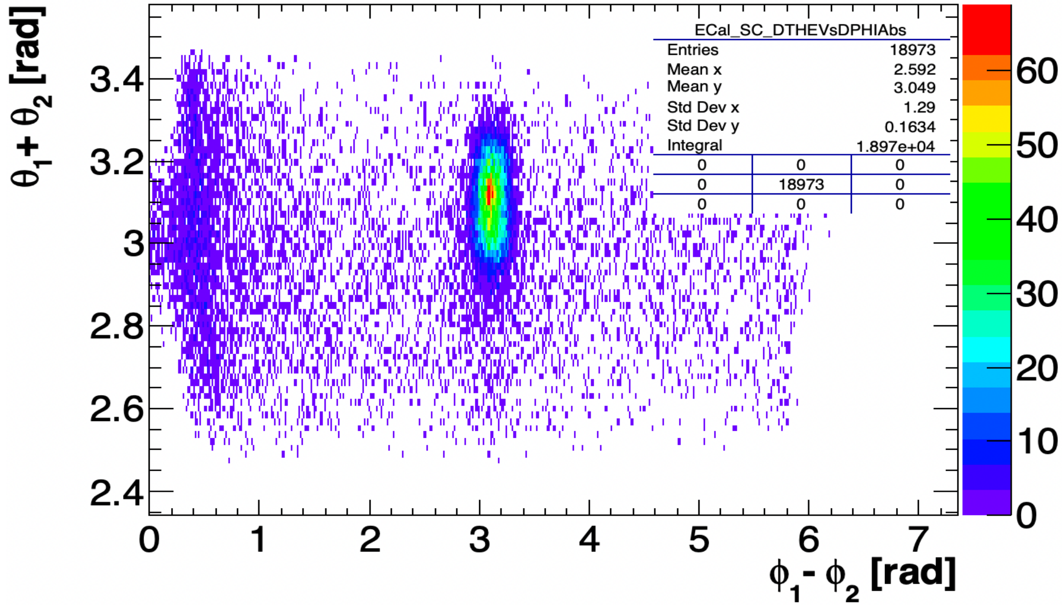

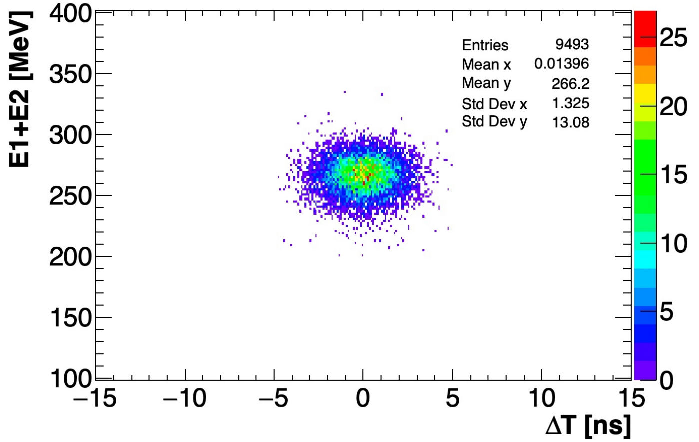

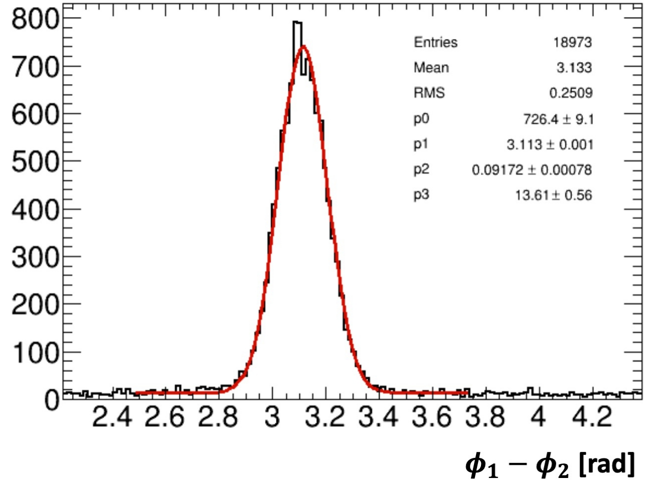

- ECal based: two in-time clusters with two body kinematics
- Background estimation: ~ 4 %
- The measurement is N_{2cl}/Flux (E_{beam})
  - Flux = PoT

Signal selection: selection efficiency

Cluster reconstruction efficiency:
TAG & PROBE with DATA

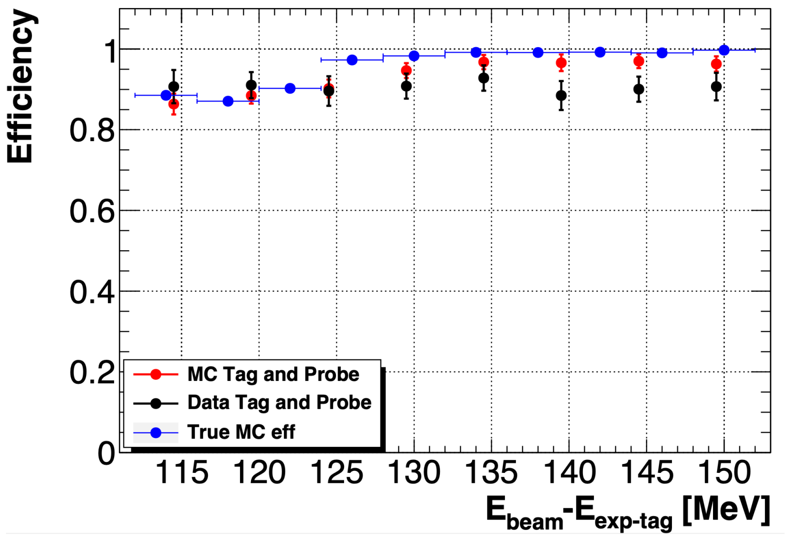

- Single hit identification threshold of 15 MeV
- Cluster reconstruction efficiency is stable over time
  - With the bad crystals excluded from the reconstruction

Geometrical efficiency (acceptance)

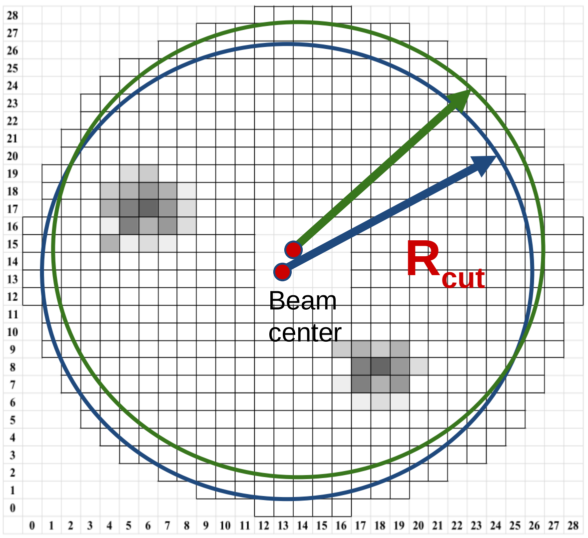

- Dominated by the cut on the outer radius of a cluster in the calorimeter
- Beam center drift limits the maximal R_{cut}

Event selection and beam position monitoring

Timepix 3 array

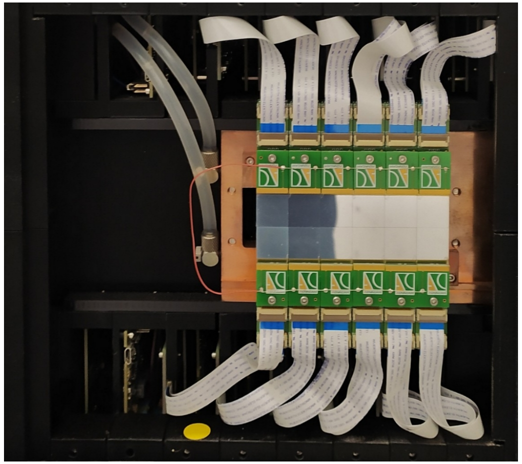

COG at the ECal front face from 2 cluster events

Movement within 10 mm

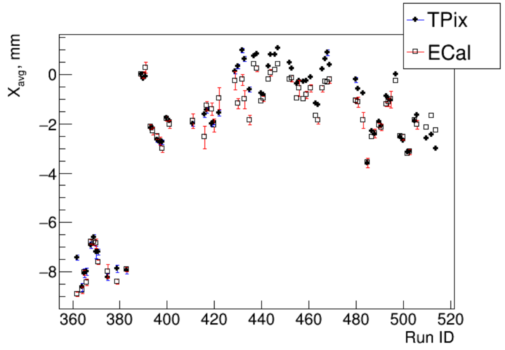

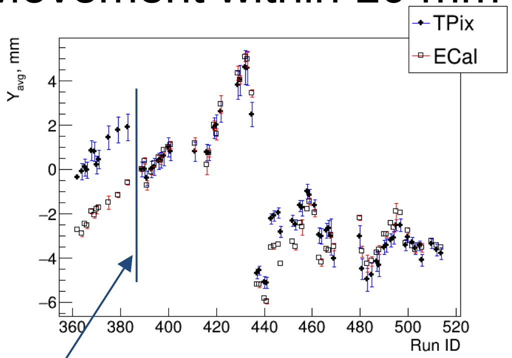

Timepix was moved by 1.8 mm

- Matrix of 2 x 6 Timepix3 detectors
  - each 256x256 pixels
- Operated in 2 modes:
  - image mode, integrating
  - streaming mode, feeding ToT and ToA for each fired pixel

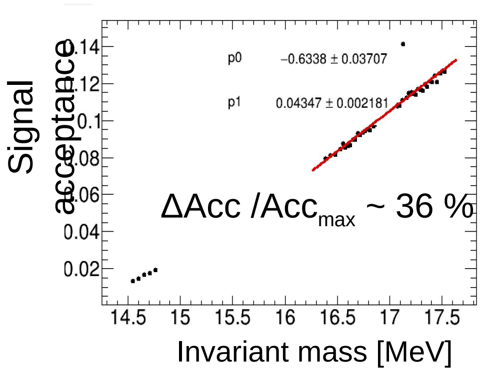

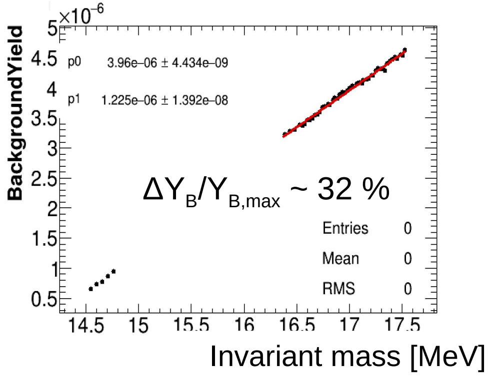

JHEP 2024, 2024(8), 121

Positron flux measurement

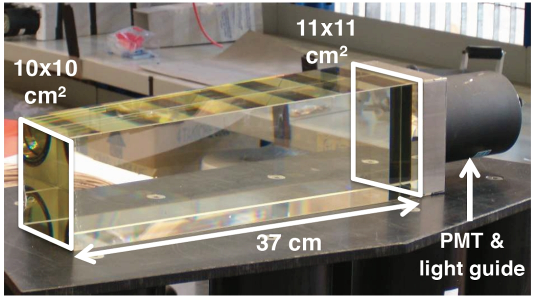

- PoT is primarily measured by an OPAL lead glass block downstream of the setup
- Additional detectors to control the PoT systematics
  - and to derive correction factors
- Several testing campaigns
  - A few positrons -> clear 1e, 2e, etc. peak identification
  - O(2000) PoT - cross-calibration with the BTF FitPix

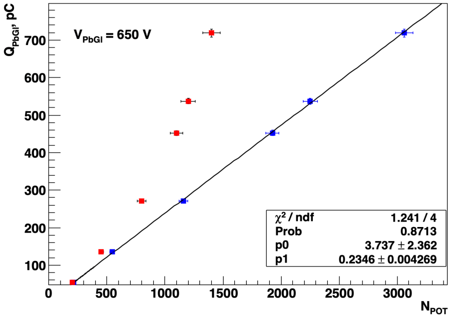

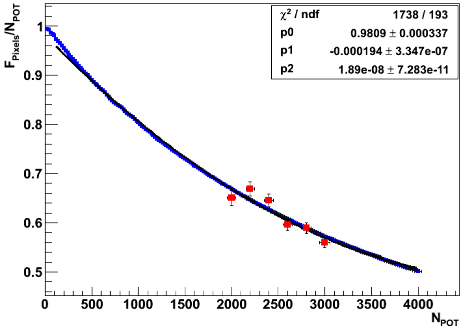

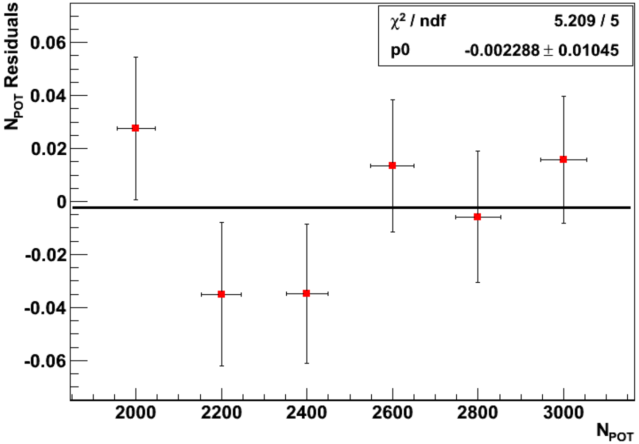

- Higher energy runs
  - control of the NPoT systematics
  - 2 clusters selection stability

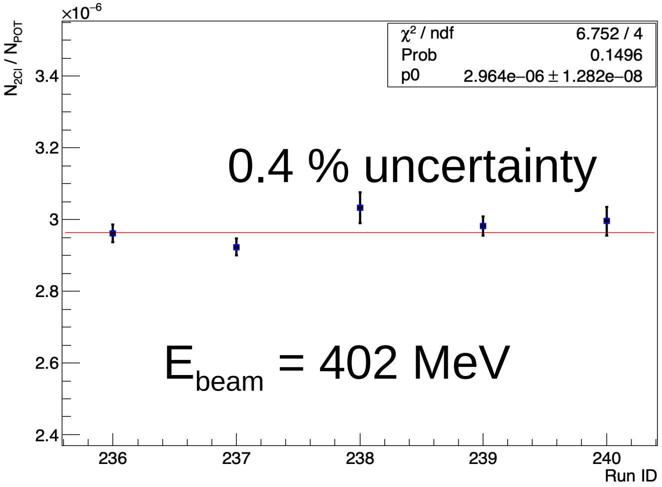

- Validation of the toy MC (and F_{pixel} correction factor) with an independent measurement from BTF luminometer
- Correction uncertainty - of the order of 1 %
  - Common to all the measurements

Sensitivity estimation

- Sensitivity depends on S/B and the uncertainty on the background determination
  - Statistical (N_B), 47 points with $O(10^{10})$ PoT, $\Delta E = 0.75$ MeV
  - Systematics (e.g. N_{poT})
  - Background: $N_B \sim 45000$ events per point
  - Signal acceptance

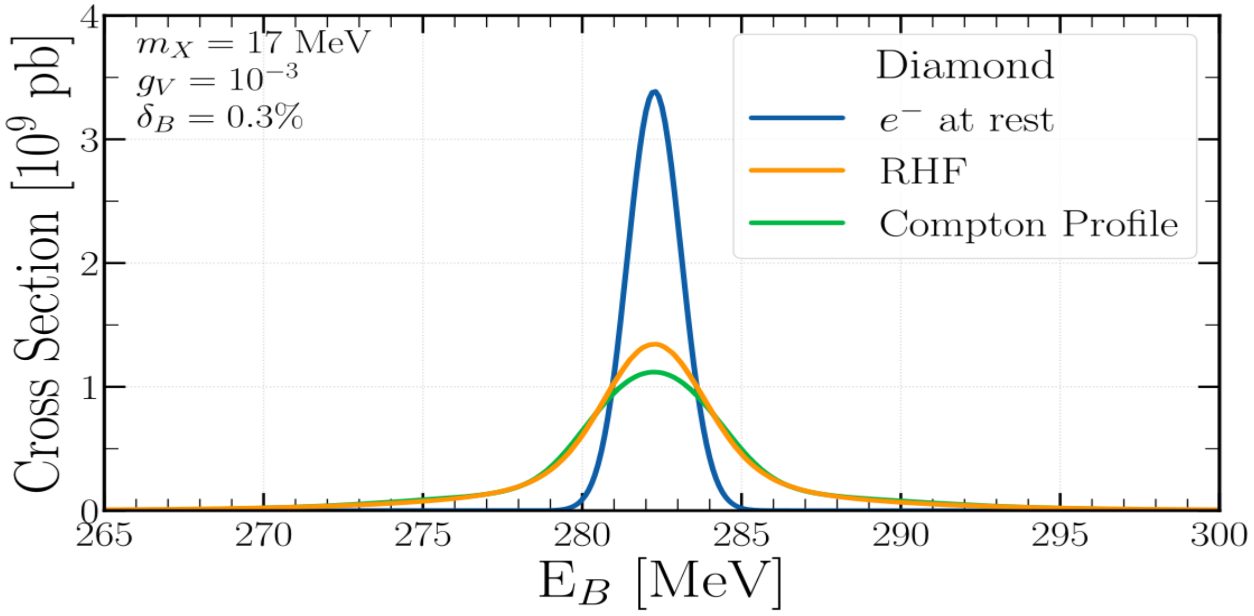

Sources of systematics

- Relative PoT estimation O(0.5%)
- Acceptance 0.75%
- Beam energy spread 0.05 %
- Signal shape uncertainty
- Beam
- Time dependent ECal efficiency
- Beam energy uncertainty - controlled by Hall probes < 10^{-3}
- ECal calibration

Normalization systematics

- absolute PoT - 5 %

PADME MC sensitivity estimate for RUN III

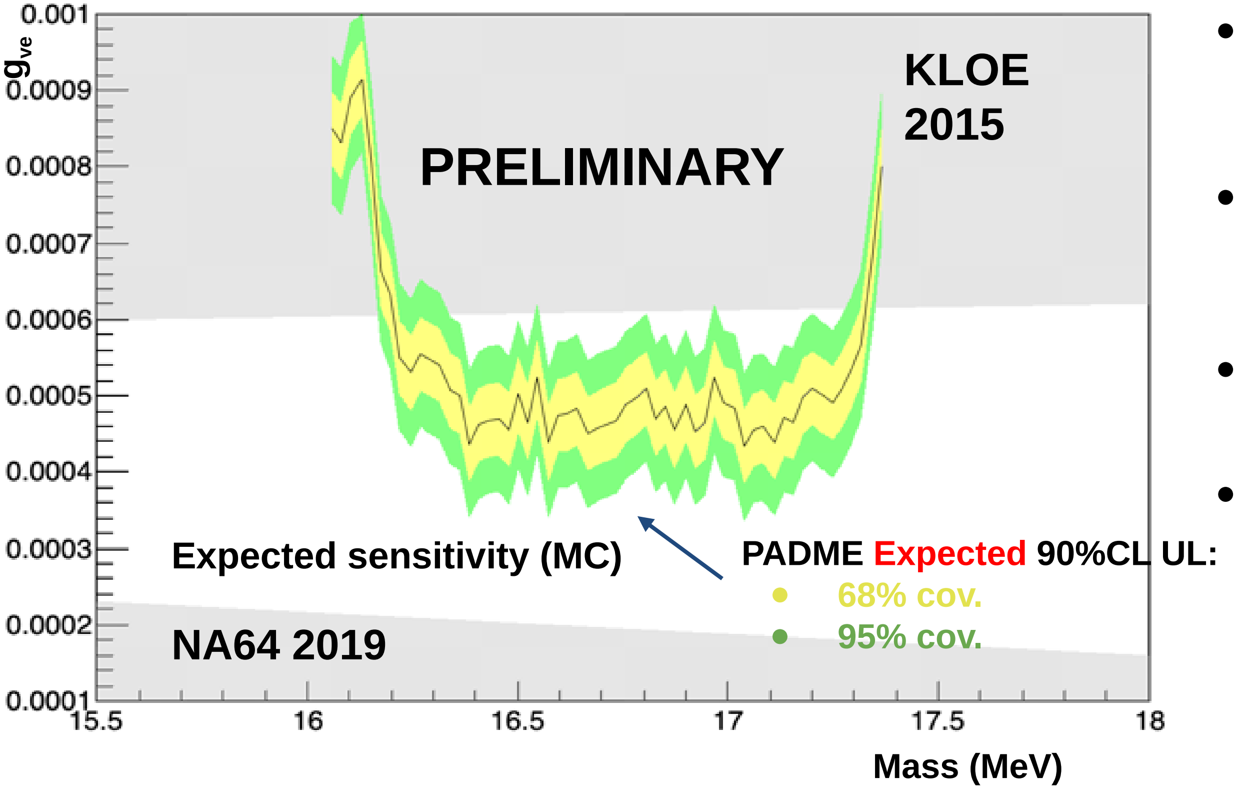

- Expected 90% CL upper limits are obtained with the CLs method
  - modified frequentist approach, LEP-style test statistic
- Likelihood fits performed for the separate assumptions of signal + background vs background only

$$Q_{statistics} = -2\, ln\, (L_{s+b} / L_b)$$

- Pseudo data (SM background) is generated accounting for the expected uncertainties of nuisance parameters + statistical fluctuations
- 150 Nuisance parameters:
  - POT of each scan point
  - Common error on POT (scale error)
  - Signal efficiency for each scan point
  - Background yield for each scan point
  - Signal shape parameters: signal yield @ a given X17 mass and g_{ve}
  - Signal shape parameter: beam-energy spread

Strategy for PADME Run IV: $N_{e+e-}/N_{\gamma\gamma}$

- The results from PADME RUN III will be dominated by PoT systematics, two clusters acceptance acceptance systematics

→ Exploit a different normalization channel which could possibly cancel part of the systematic effects

- Natural candidate: $e^+e^- \to \gamma\gamma$
    - Same 2 body kinematics: similar ECal illumination, systematics due to bad ECal crystals largely cancels

- Back on the envelope estimation: need knowledge of $N_{\gamma\gamma}$ at 0.5 % for each scanning point
    - $\sigma(e^+e^- \to \gamma\gamma)_{E=300\ MeV}$ ~ 2 mb, Acc ($e^+e^- \to \gamma\gamma$) ~ 10 % ⇒ O(10k) $\gamma\gamma$ events per 10^{10} PoT
        - Need 4 times higher statistics per scan point
    - Less scan points due to the widening of X17 lineshape because of the electronic motion
    - Higher intensity – by a factor of 2
- Need good separation between charged and neutral final states

PADME tagger

- A novel micromegas readout plane suggested
  - Rhomboidal pads for X and Y direction, decrease the mutual capacitance
- Variable HV depending on the distance from the beam center
  - Low HV in the center, measure the beam multiplicity
    - Additional control on the PoT
  - Higher HV in periphery to ensure close to 100 % efficiency

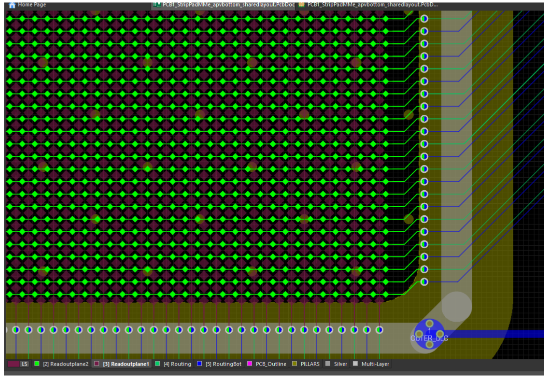

$HV_1 > HV_2 > HV_3$

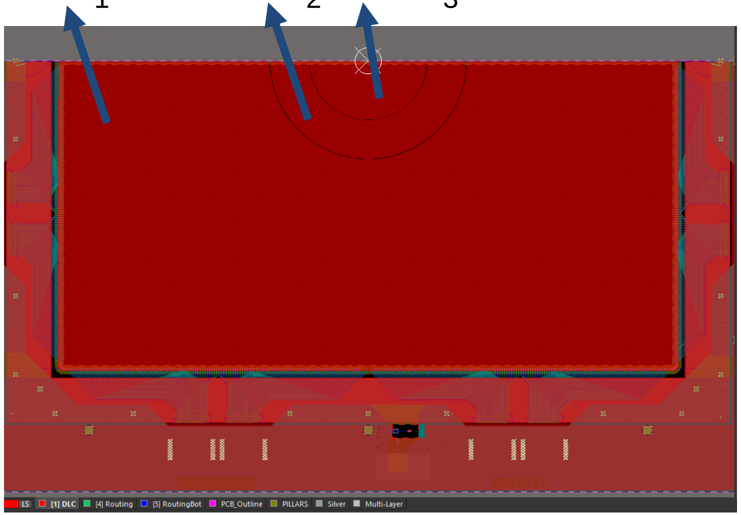

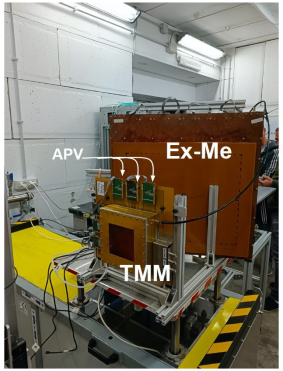

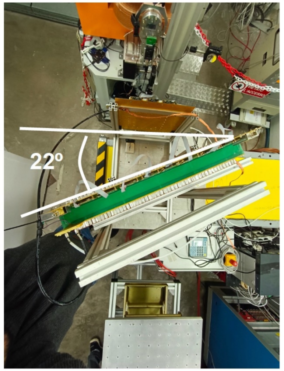

- Gas mixture: $Ar:CF_4:i\text{-}C_4H_{10} = 88:10:2$
- Readout - SRS system with APV ASIC hybrid
  - An adapter card in preparation to allow APV25 to accept/record trigger signal
  - Timing and event matching

Conclusions

- PADME Run II data used for e+e– → γγ cross section determination

- Dark photon analysis in RUN I/II data pushed forward thanks to application of ML methods for hit reconstructions in high rate environment

- X17 analysis advances by exploring the systematics
  - PoT determined with various cross-calibration procedures with uncertainty down to < 1 %
  - Signal acceptance and background estimation under control with systematics O(1%)

- A major improvement to PADME setup before RUN IV
  - Precise e^+e^- / ɣɣ discrimination with a new Micromegas tracker
  - **Allow probing the full unexplored region for the X17 allowed parameter space**